

Article

Torsional Fatigue Performance of a Spot-Welded Structure: An XFEM Analysis

Murat Demiral ^{1,*}  and Ertugrul Tolga Duran ²¹ College of Engineering and Technology, American University of the Middle East, Egaila 54200, Kuwait² Engine and Control Limited Company, BMC POWER, Teknopark İstanbul, İstanbul 34906, Türkiye; ertugrult.duran@gmail.com

* Correspondence: murat.demiral@aum.edu.kw

Abstract: This study delves into the exploration of the fatigue performance of a structure that has been spot-welded and is being loaded with torsional fatigue. The extended finite element method (XFEM) was applied to simulate the intricate interaction of spot welds in response to cyclic loading. The developed model was validated through experiments. The influences of different parameters, such as the number of spot welds used to join the adherends, the diameters of the spot welds, and the load ratio applied, on the fatigue performance of the box were investigated. The first two parameters studied had a significant influence on the extent of the fatigue failure-affected spot welds, where the crack propagation rate can be decreased by more than 700%.

Keywords: spot-welded box; XFEM; torsional fatigue loading; load ratio; the diameter of the spot weld; the number of spot weld



Citation: Demiral, M.; Duran, E.T. Torsional Fatigue Performance of a Spot-Welded Structure: An XFEM Analysis. *Appl. Sci.* **2024**, *14*, 9593. <https://doi.org/10.3390/app14209593>

Academic Editors: Nieslony Adam and Robert Owsiański

Received: 22 September 2024

Revised: 6 October 2024

Accepted: 16 October 2024

Published: 21 October 2024



Copyright: © 2024 by the authors. Licensee MDPI, Basel, Switzerland. This article is an open access article distributed under the terms and conditions of the Creative Commons Attribution (CC BY) license (<https://creativecommons.org/licenses/by/4.0/>).

1. Introduction

Spot welding is a crucial technique in the field of aerospace engineering, greatly aiding in the building and assembly of aircraft components. The lightweight and very durable materials, including titanium and aluminum alloys, that are frequently utilized in aerospace applications are one of the main causes of its significance. Spot welding makes it possible to precisely fuse these materials, forming robust and long-lasting connections that are crucial for the structural integrity of aircraft parts. The method ensures that the overall weight of the aircraft is reduced without sacrificing strength, and it is especially useful when fabricating fuselage panels, wing structures, and other crucial components. In addition to its role in material compatibility, spot welding provides benefits in terms of efficiency and speed during the manufacturing process. To achieve the high safety and performance requirements of aerospace engineering, assembly must be done precisely and consistently. Spot welding offers a quick and automated way to attach components securely while cutting expenses and manufacturing time. In order to preserve the dimensional precision of aerospace components, the method also permits targeted heating, reducing the possibility of thermal distortion in the surrounding areas. Overall, spot welding has become a preferred process in aircraft manufacturing due to its speed and precision, which helps the industry satisfy stringent quality criteria and timetables [1]. On the other hand, the operation and safety of airplanes depend heavily on sensors, thermal management systems, and electrical components. The total dependability of these systems is increased by spot welding, which guarantees strong connections between conductive materials. For electrical components to function efficiently and to help minimize any failures that could jeopardize the performance of crucial aeronautical systems, the technique's ability to build consistent, low-resistance junctions is vital [2].

In operational conditions, mechanical components of the structures, including aerospace ones, typically undergo cyclic loading, making the prevention of fatigue failure a primary design consideration. Given that spot welds establish localized connections, forming inherent

circumferential notches, they result in stress concentrations, thereby increasing the likelihood of structural failure due to fatigue. For example, in automotive components, fatigue failures often arise in the region of a spot weld around 80% of the time, at a low-quality cut edge 15% of the time, and fatigue cracks in sheet metal just 5% of the time [3]. Thus, it can be concluded that spot-weld joints' fatigue strength has a major impact on the overall structural durability under typical service conditions. Therefore, a deeper understanding of spot-weld fatigue behavior and the application of reliable fatigue assessment models have to be considered necessary conditions for guaranteeing trustworthy designs.

In the literature, there exist a few studies focused on the cycling performance of spot-welded structures. For instance, Ertas et al. [3] investigated the fatigue failure of modified tensile-shear specimens using experimental and numerical methods. It focused on auto-mated and manual spot-weld joints, applying various load ranges during fatigue tests. Results showed that manually spot-welded specimens had 30–45% fewer cycles to failure than automated joints. Microscopic examination revealed gaps in manual spot-weld nuggets, but fatigue-induced cracks consistently formed on their peripheries, similar to automated joints. This difference was attributed to stress concentrations from unsymmetrical weld geometry. In another study, using the Coffin-Manson model, Ertas et al. [4] investigated fatigue life in spot-weld joints, taking into account varying spot-weld diameters and sheet thicknesses. The study revealed that fatigue life depended on joint type, load amplitude, sheet thickness, and spot-weld diameter. Larger diameters and thicknesses correlated with longer fatigue lives within certain limits, but beyond a threshold, increased thickness did not improve fatigue strength. Notably, using a greater number of small spot welds was more effective in enhancing fatigue strength compared to larger spots with equivalent cross-sectional areas. Effertz et al. [5] performed fatigue tests on specimens welded with friction spot welding using a stress ratio of $R = 0.10$. The two-parameter Weibull distribution was used to statistically examine the fatigue life of the linked overlapped sheets. The findings demonstrate that an infinite life of the service component can be attained at a comparatively low load, equivalent to 10% of the maximum supported by the joint. It was observed that circumferential cracking propagated around the spot-welded zone for high loads. On the other hand, for lesser loads, the crack spreads circumferentially around the weld nugget; however, because insufficient solicitation occurred to boost plastic deformation in the weld nugget, the fracture tended to spread in the direction of width. Similar research was done by Plaine et al. in experimental research [6], which looked at the fatigue behavior of a single friction spot welded of Ti6Al4V and AA5754 dissimilar structures. In the specimens, two fatigue failure modes were noted. The upper aluminum sheet failed under high cycle loads because of increased stress concentration at the notch tip, which caused a fracture to initiate and propagate through the thickness towards the joint surface. Under low cyclic load, a "through weld" failure was noted, as the crack rapidly spread over the interfacial surface until reaching a critical point where the remaining cross-section could not withstand the shear overload, resulting in failure. The impact of varying nugget diameters on the fatigue lifetimes of distinct welded joints of Dual-Phase (DP) 800 and Twinning-Induced Plasticity (TWIP) 1000 steel was investigated by Doruk et al. [7]. Duran and Demiral [8] compared and validated the numerical modeling of fatigue failure of spot-welded joint using the finite element method (FEM) and extended FEM (XFEM) for high cycle fatigue. In Nikolic et al.'s investigation [9], the fatigue service life of an interface crack between two elastic layers was evaluated using the Paris law and the linear elastic fracture mechanics concept. Demiral and Duran [10] analyzed the fatigue failure of the spot-welded structure subjected to tensile loading using XFEM for different values of the cyclic load, the load ratio, and nugget size.

In aerospace applications, due to various factors and operational conditions, torsional loadings frequently occur. For instance, during flight maneuvers such as rolls and turns, different parts of an aircraft experience torsional loads, such as the wings, which are subjected to twisting forces as the aircraft changes its orientation. Also, changes in airflow and aerodynamic forces can induce torsional loads on aircraft components, where the

wings, control surfaces, and other protruding elements are exposed to varying wind conditions during flight, leading to torsional stresses. Structural asymmetry in an aircraft, whether intentional or due to design constraints, can lead to uneven distribution of loads, including torsional forces. Atmospheric turbulence, sudden changes in wind direction, and ground-related forces during landing and taxiing are other factors that may lead to the presence of torsional loadings. The performance of spot-welded structures subjected to torsional loading used in aerospace applications needs to be addressed during its design considerations. In the literature, only one study was investigated. Three different spot weld modeling approaches—rigid, solid element, and umbrella spot welds—that use static and multiaxial low cycle torsional fatigue analysis were the focus of Duran et al.'s study [11]. The highest stress values and lowest fatigue life cycles are seen outside the nugget boundary in rigid and umbrella weld models. Conversely, with higher weld diameters, the critical region moves outside the nugget boundary with reduced stress and increased life. For smaller spot weld diameters, the solid element modeling technique results in maximum stress and minimal life inside the weld zone.

The review articles on spot-welded structures [12–15] and the literature survey indicate a need for an in-depth study of a spot-welded structure under torsional fatigue loading. It helps to increase fatigue resistance and increase the service life of spot-welded assemblies to fully understand the failure causes. It is crucial to understand the location of fracture initiation, how it spreads with increasing cycling loadings, the failure cycle, and how these factors depend on design parameters. The XFEM model for the spot-welded structure subjected to torsional loading is constructed in this study with this goal in mind. The XFEM approach is very useful for capturing complex crack patterns since it can simulate the propagation of cracks without changing the mesh, whereas most studies in the literature combined FE models with fatigue theories to determine the fatigue life of a spot-welded component without capturing intricate crack formations and their spreads. First, in this work, the experimental data for two distinct scenarios were used to validate the numerical model. Afterwards, an evaluation was conducted to determine how different model parameters, such as the nugget diameter, load ratio, and quantity of the applied loading, affected the fatigue life assessment of spot-welded components.

2. XFEM Modelling

In this study, XFEM, linear elastic fracture mechanics, and Paris Law were integrated together to simulate fatigue crack growth. In XFEM analysis, a displacement vector function u with the partition of unity enrichment is approximated as:

$$u(x) = \sum_{I \in N} N_I(x) \left[u_I + H(x)a_I + \sum_{\alpha=1}^4 F_{\alpha}(x)b_I^{\alpha} \right] \quad (1)$$

where $N_I(x)$ represents the typical nodal shape functions; u_I , the typical nodal displacement vector associated with the continuous portion of the finite element solution, is the first term on the right-hand side of the above equation. The second term in the equation is the result of multiplying the nodal enriched degree of freedom vector (a_I) by the associated discontinuous jump function $H(x)$ across the crack surfaces. The third term is the product of b_I^{α} , the nodal enriched degree of freedom vector, and the related elastic asymptotic crack-tip functions $F_{\alpha}(x)$. Here, all of the nodes in the model are covered by the first term on the right; nodes whose shape function support is cut by the crack interior only fall under the second term; and nodes whose shape function support is cut by the crack tip only fall under the third term. Additional information on it can be obtained elsewhere [16].

Figure 1a shows a three-dimensional XFEM model of the spot-welded box profile under torsional loading. It was developed using Abaqus 6.14. The box was subjected to the torsional loading from one end with a length of 70 mm, while the other end with the same size was fixed in all directions. This load was applied to the reference point shown in Figure 1a, located at the geometrical center of the loaded part of the box, and this point was

controlling the concerned region through the coupling constraint defined as in the software. XFEM was defined as every point of both adherends joined together. To simulate spot welding, the interfaces of the two adherends on the welding side were specified as master and slave surfaces using the tie constraint module included in Abaqus. The dimensions of the XFEM model are shown in Figure 1a. These dimensions were selected based on those of experiments performed in [11,17]. The model was validated using these experimental results. A brief self-descriptive equation used in XFEM calculations is presented in Table 1. Its details can be found elsewhere [8,16]. To replicate the fatigue loading, a direct cyclic analysis was performed using 25 Fourier terms (to directly acquire the stabilized cyclic response, the direct cyclic technique combines a modified Newton approach with a Fourier representation of the solution and the residual vector). In order to induce crack formation at the stress concentration areas, T_{\max} (the maximum torque value applied in the fatigue analysis) was used in a static stage prior to the loading cycle.

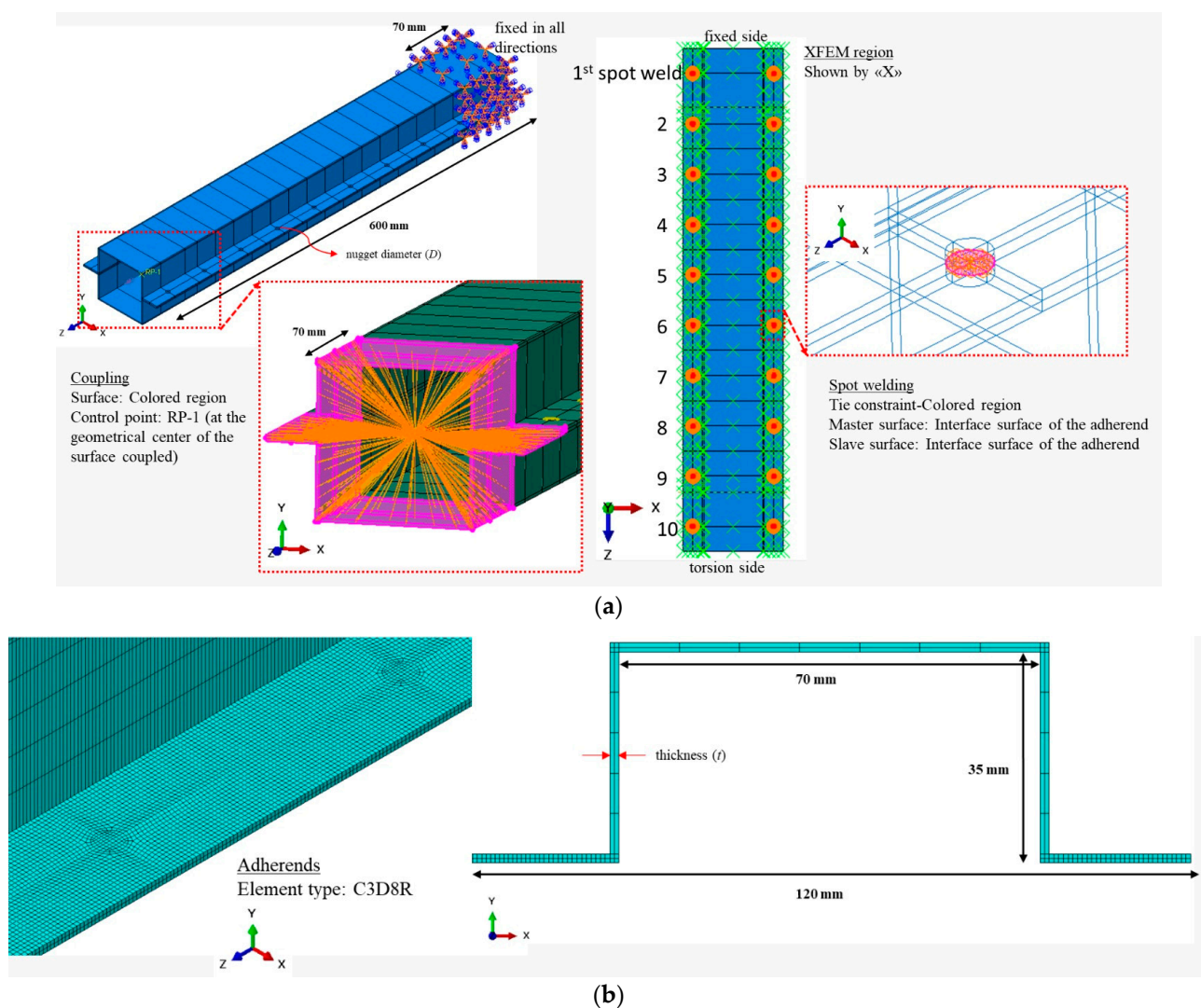


Figure 1. Details about the XFEM model of a spot-welded box exposed to torsional fatigue loading (a) and the FE mesh used in the analysis (b).

Details of the mesh used in the model are presented in Figure 1b. A finer mesh was utilized in the welding region, while a coarser one was considered in the other portions of both adherends. To ensure accuracy of the model, a mesh convergence study was performed. Three simulations with three different mesh sizes, namely 0.000375 mm, 0.000750 mm, and 0.0015 mm, were performed when the box was subjected to static T_{\max} loading. The maximum von Mises stress value obtained from each model, observed in the element next to the welding regions, was compared. The concerned change was less than 3.5% when the mesh size was changed from 0.00075 mm to 0.000375 mm, which was more than 10.0% when the mesh was changed from the coarsest one into the medium one. The model was therefore discretized with an element size of 0.00075 mm. It is worth mentioning at this point that when the coarsest mesh with an element size of 0.0015 mm was used in the model, the location of the onset of the crack was entirely incorrectly predicted (see Figure 2). The experimental studies in the literature showed that the cracks in the structure emerged around the spot-welding regions. This was captured in our simulations whenever a finer mesh was used. Eight-noded linear brick elements with reduced integration (C3D8R) were used in the discretization. The material constants for 1010A hot rolled steel used in the simulations are as follows: $E = 210,000$ MPa, $\nu = 0.3$, and $\sigma_{\max} = 326$ MPa [11], $G_{1c} = G_{2c} = G_{3c} = 6500$ N/m [18], $c_3 = 7.5 \times 10^{-8}$ and $c_4 = 1.75$.

Table 1. Definitions and equations used in XFEM analysis [16].

Equation	Description and Definition
$G_{pl} = 0.85 G_{eq, c}$	G_{pl} : the maximum energy release rate $G_{eq, c}$: the critical equivalent strain energy release rate
$G_{thresh} = 0.01 G_{eq, c}$	G_{thresh} : the lower limit for the strain energy release rate
Mixed mode power law model $\frac{G_{eq}}{G_{eq, c}} = \left(\frac{G_1}{G_{1c}}\right)^{\alpha_1} + \left(\frac{G_2}{G_{2c}}\right)^{\alpha_2} + \left(\frac{G_3}{G_{3c}}\right)^{\alpha_3}$	G_{1c} , G_{2c} and G_{3c} : the critical energy release rates in the opening (Mode I), first shear (Mode II), and second shear (Mode III) modes G_1 , G_2 and G_3 : the resulting energy release rates in the opening (Mode I), first shear (Mode II), and second shear (Mode III) modes in the course of deformation α_1 , α_2 and α_3 : the coefficients used in the power law (all taken to be 1.0)
Paris Law $da/dN = c_3 \Delta G^{c_4}$	a : the crack length N : the cycle number da/dN : the crack propagation rate c_3 and c_4 : the material constants ΔG : the difference in energy release rates when the minimum and maximum loads applied
$G_{pl} > \Delta G > G_{thresh}$	this inequality to be satisfied for the validation of Paris Law G_{pl} : the strain energy release rate upon the plastic deformation starts
$\Delta a_{Nj} = a_{N+\Delta N} - a_N$	a_N : the crack length from the current cycle $a_{N+\Delta N}$: the crack length after ΔN cycle increment Δa_{Nj} : the change in crack length based on the number of cycles needed for the crack to propagate over its element length
$\Delta N_{min} = \min(\Delta N_j)$	the node j representing the node corresponding to the crack tip that required the least number of cycles for propagation ΔN_{min} : the least number of cycles for propagation
$\Delta a_{Nmin} = \min(\Delta a_{Nj})$	the change in crack length based on ΔN_{min}

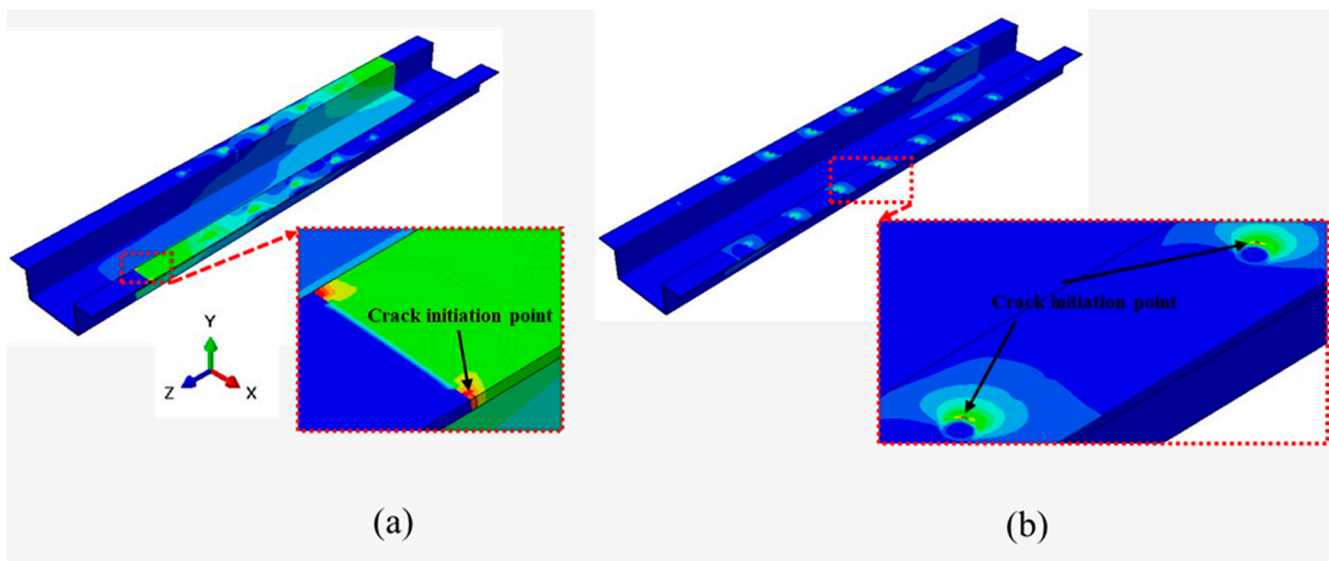


Figure 2. The resulting crack initiation sites when coarse (a) and medium (b) mesh sizes were used in the simulations.

3. Results and Discussion

In this section, the underlying deformation mechanisms of the spot-welded box subjected to torsional loading were investigated. Figure 3 demonstrates the deformed shapes of the box with displacement profile when it was subjected to min ($T_{\min} = -T$) and maximum ($T_{\max} = T$) loadings for $R = -1.0$. While the displacements are reaching their maximums at the side torsioned, those of another end are 0. In the simulations, it was observed that the spot-welding spots on the overlapping surfaces of the welded box served as the cracks' nucleation point, and as the structure underwent cyclic loads, they subsequently spread out along its width. Here, the cracks mainly emerged at the spot-welded twins' at the fifth and sixth rows from the fixed side. The cracks formed at the overlapping surfaces reached the free surfaces after a significant number of cycles. Figure 4 depicts the cracks nucleated at the overlapping and free surfaces of the upper and lower adherends when $R = 0$ at 500,000 cycles. Obviously, the cracks formed and expanded at the joined surfaces of the upper and lower adherends more significantly than those at the free surfaces.

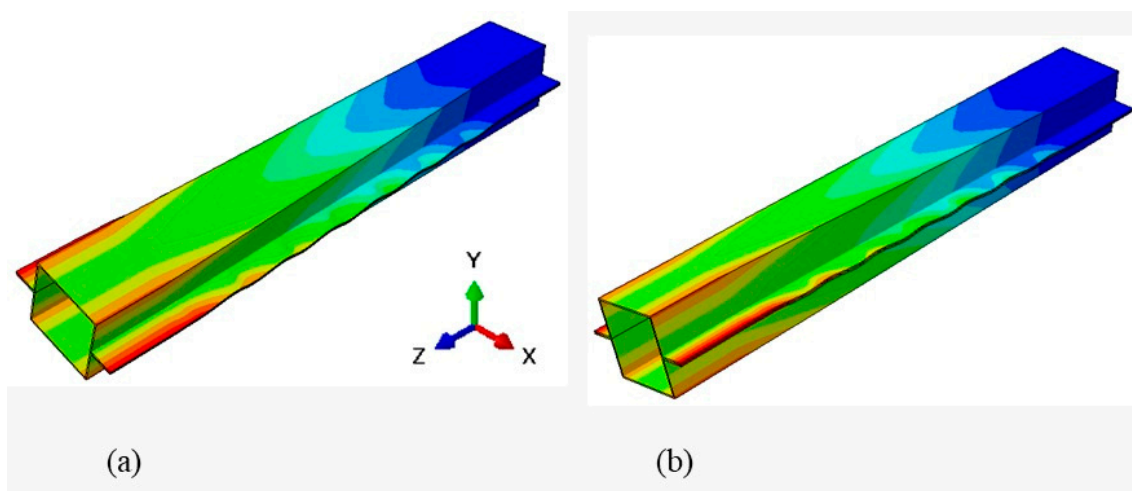


Figure 3. Deformed shape of the spot-welded box when $T_{\min} = -T$ (a) and $T_{\max} = T$ (b) was applied during fatigue torsional loading (deformation was scaled 100 times for better visualization).

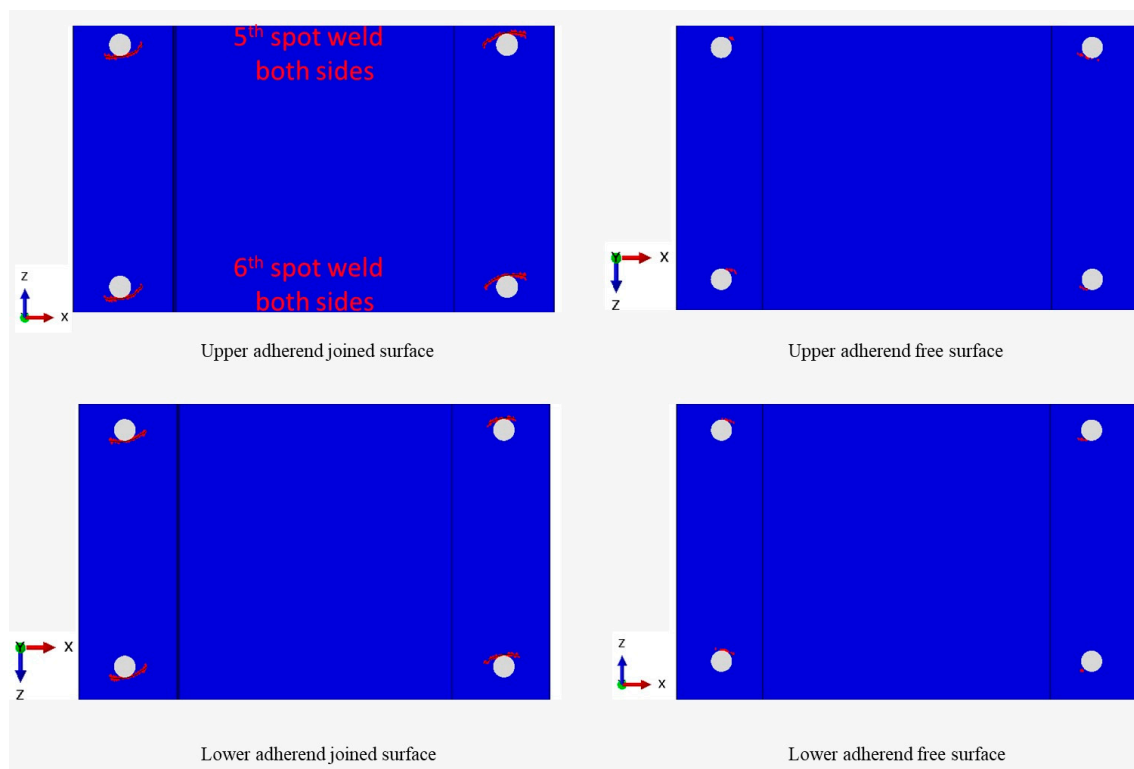


Figure 4. The illustration of the cracks that spread around the spot weld at the top and lower adherends' overlapping and opposing surfaces at $N = 500,000$ cycles ($R = 0.0$).

For the validation of the developed XFEM model of the spot-welded box torsioned, the experimental data presented in [17] were used. Apart from the box with the geometry presented in Section 2, a thicker adherend twin with 2.0 mm thickness, where they are joined with 6.5 mm diameter spot welds was also considered. Experimentally and numerically obtained failure cycles (N_f) are presented in Table 2. In the simulations, N_f was taken to be the number of cycles at which the crack length reached the nugget diameter. Overall, experimentally and numerically obtained failure cycles for two different configurations are matching each other. That validates the developed numerical model. That also shows the accuracy of the selected material constants c_3 and c_4 . The work in [17] also indicated that the 5th and 6th spot weld twins were the two most critical locations subject to fatigue failure. Ref. [17] shows the experimentally observed crack evolved around the 5th spot welding; this agrees pretty well with our conclusions, which are shown in Figure 4. It is worth mentioning that internal/residual stresses and variations in temperature and microstructural characteristics of the material introduced during the welding process were not taken into account while modeling the spot-welds.

Table 2. Experimentally and numerically obtained failure cycles for two different cases.

t	D, T	Experiments [17]	XFEM
		N_f	
1.5 mm	5.5 mm, ± 225 Nm	45,834	42,375
2.0 mm	6.5 mm, ± 320 Nm	28,000	26,950

In this work, different model parameters were varied to explore the fatigue behavior of spot-welded box torsioned. They are mainly the total number of welds used in the joining, the nugget diameter (D), and the load ratio (R).

3.1. Influence of the Total Number of Spot Welds

The total number of spot welds is one of the important parameters affecting the performance of the box. This study examined five distinct cases with eight, nine, ten, eleven, and twelve spot weld twins. Table 3 presents the obtained respective N_f and crack propagation rate (da/dN) values. They were 23,606, 27,466, 42,375, 176,660, and 10^6 cycles when the number of spot weld twins was increased from 8 to 12, where the relative changes between them were 16.3%, 54.28%, 417%, and 566%. It was seen that when an additional spot weld twin was added to the box, its effect kept increasing. Finally, it was observed that no fatigue failure was observed for 12 spot weld twins, as no crack nucleation was observed throughout the joined sample. Fatigue life larger than 10^6 cycles was regarded as the run-out in this investigation. It was concluded that it was possible to eliminate the fatigue failure in such boxes when they were subjected to torsional loading by increasing the number of spot welds. The average crack propagation rate was observed to increase from 3.10×10^{-5} mm/cycle to 2.33×10^{-4} mm/cycle, more than 7.5 times when the number of spot weld twins was decreased from 11 to 8. Figure 5 shows the crack patterns around spot welds for each configuration when N reaches to N_f . It was observed that the two central spot welds were subjected to fatigue failure when the number of spot weld twins was 8 and 10, while there were three central welding regions for the others. It appeared to be that for 9 and 11 spot weld twins, the central spot-welded region (5th and 6th rows from the fixed end, respectively) could not compensate for the whole fatigue deformation, the closer two spot weld twins were also subjected to the failure. Here it was concluded that for the given loading amount, the central two and three spot weld twins accommodate the fatigue failure for the even and odd numbers of the total number of spot weld twins, respectively. Obviously, for a larger amount of loading provided that it does not result in plastic deformation, the fatigue deformation expands from the central twins to the ones located around them.

Table 3. Numerically obtained N_f and da/dN for different assembly configurations ($t = 1.5$ mm).

Number of Spot Weld Twins	D (mm)	R (mm)	N_f (Cycle)	da/dN (mm/Cycle)
8	5.5	−1.0	23,607	2.33×10^{-4}
9			27,466	2.00×10^{-4}
10			42,375	1.30×10^{-4}
11			177,660	3.10×10^{-5}
12			10^6	-
10	4.5	−1.0	20,524	2.2×10^{-4}
	5.5		42,375	1.30×10^{-4}
	6.5		211,845	3.07×10^{-5}
10	5.5	−1.0	42,375	1.30×10^{-4}
		0.0	48,058	1.14×10^{-4}
		0.5	93,900	5.85×10^{-5}

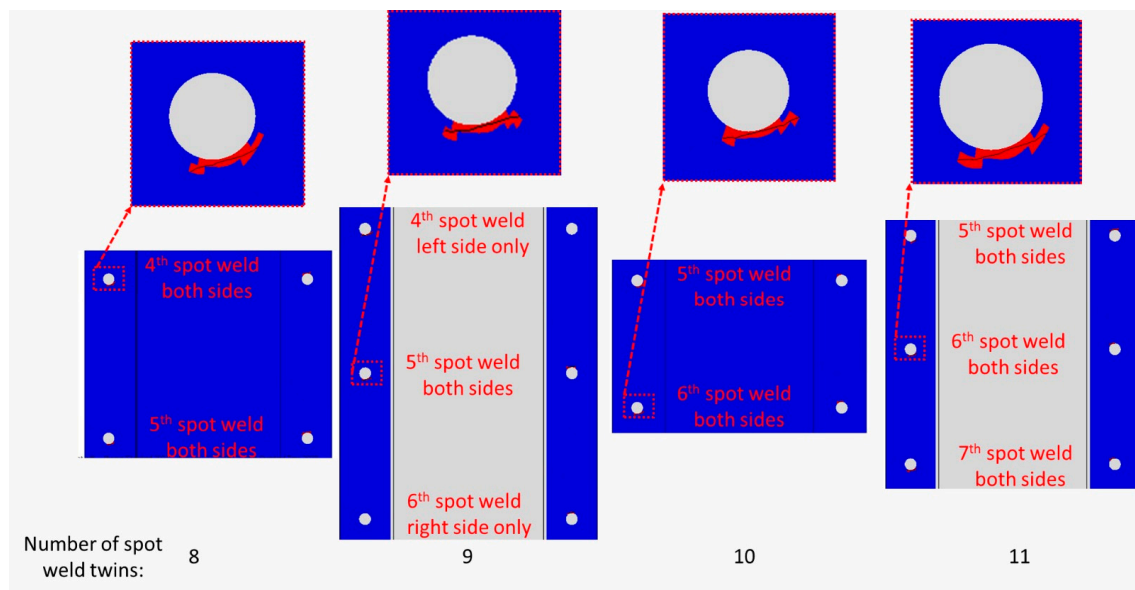


Figure 5. The depiction of the cracks that spread around the spot weld at the bottom adherends' overlapping surface for different numbers of spot weld twins at $N = N_f$.

3.2. Influence of Nugget Size

Second, an analysis was conducted to determine the impact of the spot weld's diameter on the spot-welded box's fatigue life. This size was adjusted for this reason, going from 4.5 mm to 6.5 mm in increments of 1.0 mm. Table 3 presents the obtained N_f values, where they are 20,524, 42,375, and 211,845 cycles, respectively. When the diameter of the spot-welded region was increased, N_f increased. This result brings us to the point that an infinite fatigue life could be attained for the box studied when D is increased to 7.5 mm or 8 mm. On the other hand, the average crack propagation rate decreased by more than 7 times from 2.2×10^{-4} to 3.07×10^{-5} mm/cycle when D was increased from 4.5 to 6.5 mm. Figure 6 presents the resulting fatigue failure patterns. While the cracks originated and propagated at the central four spot weld twins when D equaled to 4.5 mm, it was only the 6th spot weld twin itself that accommodated the overall failure. Here, it was concluded that the spot weld's size had a major impact on the box's fatigue performance. This is consistent with the discovery in [4,19], where longer fatigue lifetimes were obtained by the bigger nugget diameter due to the notch effect, which led to reduced strains and stresses evolving near the spot-welding site; hence the cracks could originate less possibly.

3.3. Influence of R

One of the crucial factors that could affect a box's torsional fatigue performance is the load ratio. In this section, its effect was analyzed, where three different load ratios R were considered, namely -1.0 , 0.0 , and 0.5 . Table 3 shows the obtained N_f values. It was observed that there were 42,375, 48,058, and 93,900 cycles for R equaled to -1.0 , 0.0 , and 0.50 , respectively. It was noticed that the change was not significant when R changed from -1.0 to 0.0 , but this change was noticeable when R became 1.0 . As R is the ratio between T_{\min} and T_{\max} and their difference characterizes the fatigue loading, for R equaled to 0.5 , the stress levels during the cyclic loading were not as significant as R equaled to 0.0 or 1.0 , and the life span of the structure increased around two times. Parallel to this, its average crack propagation rate (5.85×10^{-5} mm/cycle) was almost half of the others. Figure 7 presents the cracks around spot welds for each case when N_f was reached. For all of them, the identical spot weld twins experienced the fatigue failure. That concludes that the load ratio does not affect the failed region of the box when subjected to torsional loading.

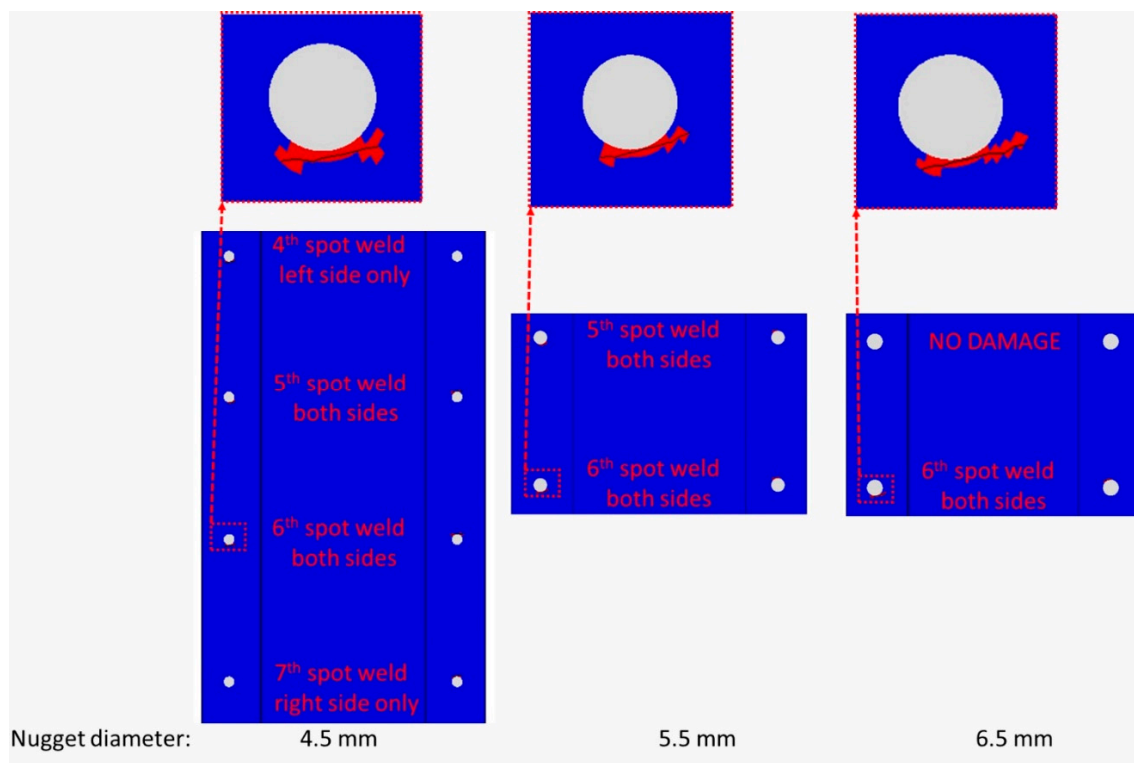


Figure 6. The depiction of the cracks that spread around the spot weld at the bottom adherends' overlapping surface for different diameters of spot weld twins at $N = N_f$.

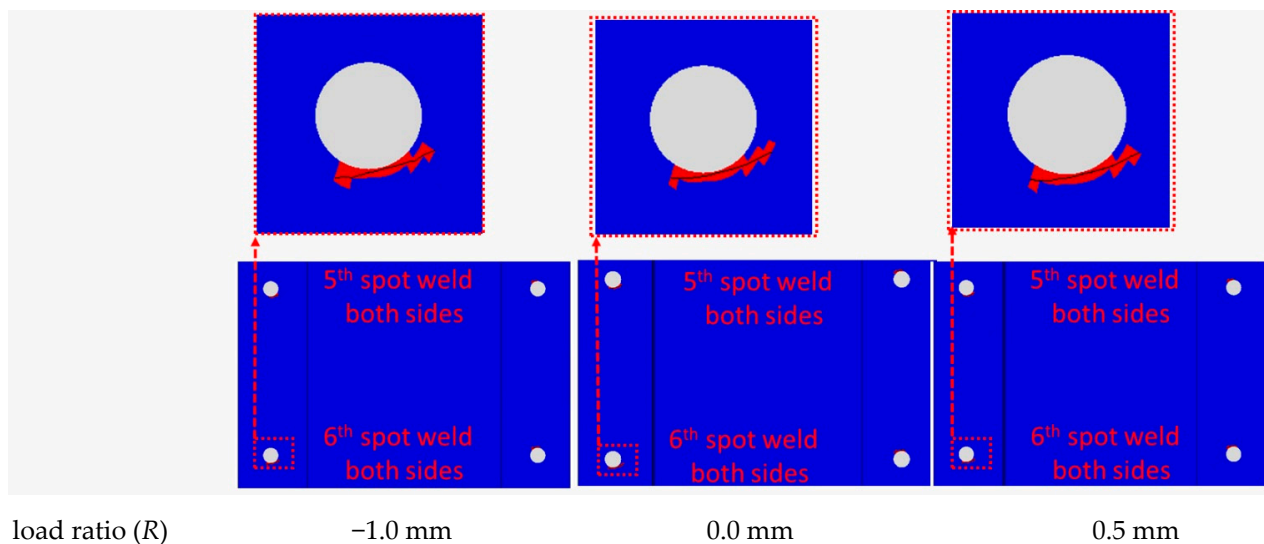


Figure 7. The depiction of the cracks that spread around the spot weld at the bottom adherends' overlapping surface for different load ratios at $N = N_f$.

4. Conclusions

The number of spot weld twins, the spot-welding diameter, and the load ratio were among the important parameters that were investigated in this computational analysis to determine the fatigue failure of the spot-welded box subjected to torsional loading. The XFEM modeling technique was employed to model the propagation of cracks. Using the experimental findings from the literature, the model was verified. Deductions were made as follows:

- The cracks began to spread throughout the structure's width from the spot-welding locations of the overlapping surfaces of the box. After a significant number of torsion cycles, these cracks spread to the adherends' opposing surfaces.
- The mesh size was found to affect the crack initiation sites significantly, especially the one in the thickness direction. When a rather coarse mesh was employed, the cracks did not start near the spot-welding locations but in other incorrect locations.
- When the total number of spot weld twins is even or odd, respectively, the central two or three spot weld twins accommodate the fatigue failure for the studied torsional fatigue loading. When this number was increased from 8 to 11, the N_f increased 7.5 times.
- When the diameter of all the spot welds was raised by 44%, the average crack propagation rate dropped by more than seven times. Also, less area around the spot welds was exposed to the fatigue failure.
- The failure cycle of the box under torsional loading is influenced by the load ratio; nevertheless, the size of the failed region of the structure remains unaffected.
- It is possible to accomplish the infinite fatigue life of the box subjected to torsional motion by adjusting the parameters studied here.

This study's conclusions provide valuable information for improving the manufacturing and design of spot-welded joints in structures, including the aeronautical ones. Also, this research advances the longevity, structural integrity, and dependability of components, ultimately supporting the overall safety and performance of systems by deepening our understanding of fatigue performance.

Author Contributions: Conceptualization, M.D.; Methodology, M.D. and E.T.D.; Validation, M.D.; Formal analysis, M.D.; Investigation, M.D.; Writing—original draft, M.D.; Writing—review & editing, E.T.D. All authors have read and agreed to the published version of the manuscript.

Funding: This research received no external funding. The APC was funded by the American University of the Middle East, Kuwait.

Institutional Review Board Statement: Not applicable

Informed Consent Statement: Not applicable

Data Availability Statement: The raw data supporting the conclusions of this article will be made available by the corresponding authors on request.

Conflicts of Interest: Author Ertugrul Tolga Duran was employed by the company Engine and Control Limited Company. The remaining authors declare that the re-search was conducted in the absence of any commercial or financial relationships that could be construed as a potential conflict of interest.

References

1. Verspeek, S.; Ribbens, B.; Maldague, X.; Steenackers, G. Spot weld inspections using active thermography. *Appl. Sci.* **2022**, *12*, 5668. [\[CrossRef\]](#)
2. He, D.; Yang, K.; Li, M.; Guo, H.; Li, N.; Lai, R.; Ye, S. Comparison of single and double pass friction stir welding of skin-stringer aviation aluminium alloy. *Sci. Technol. Weld. Join.* **2013**, *18*, 610–615. [\[CrossRef\]](#)
3. Ertas, A.H.; Vardar, O.; Sonmez, F.O.; Solim, Z. Measurement and Assessment of Fatigue Life of Spot-Weld Joints. *J. Eng. Mater. Technol.* **2008**, *131*, 011011. [\[CrossRef\]](#)
4. Ertas, A.H.; Sonmez, F.O. A parametric study on fatigue strength of spot-weld joints. *Fatigue Fract. Eng. Mater. Struct.* **2008**, *31*, 766–776. [\[CrossRef\]](#)
5. Effertz, P.S.; Infante, V.; Quintino, L.; Suhuddin, U.; Hanke, S.; Dos Santos, J.F. Fatigue life assessment of friction spot welded 7050-T76 aluminium alloy using Weibull distribution. *Int. J. Fatigue* **2016**, *87*, 381–390. [\[CrossRef\]](#)
6. Plaine, A.H.; Suhuddin, U.F.; Alcântara, N.G.; Dos Santos, J.F. Fatigue behavior of friction spot welds in lap shear specimens of AA5754 and Ti6Al4V alloys. *Int. J. Fatigue* **2016**, *91*, 149–157. [\[CrossRef\]](#)
7. Doruk, E.; Findik, F.; Pakdil, M. Mechanical and fatigue behavior of resistance spot welded dual-phase and twinning-induced plasticity steel joints. *J. Aerosp. Eng.* **2022**, *35*, 04022007. [\[CrossRef\]](#)
8. Duran, E.T.; Demiral, M. Comparing and validating the numerical modeling of spot-welded fatigue failure using FEM and XFEM methods for HCF. *Eng. Fail. Anal.* **2024**, *158*, 108049. [\[CrossRef\]](#)

9. Nikolić, R.R.; Djoković, J.M.; Hadzima, B.; Ulewicz, R. Spot-weld service life estimate based on application of the interfacial crack concept. *Materials* **2020**, *13*, 2976. [[CrossRef](#)] [[PubMed](#)]
10. Demiral, M.; Duran, E.T. Failure Analysis of Resistance Spot-Welded Structure Using XFEM: Lifetime Assessment. *Appl. Sci.* **2023**, *13*, 10923. [[CrossRef](#)]
11. Duran, E.T. Finite element based Multi-Axial low cycle fatigue analyses of Spot-Welded components and correlation with tests. *Eng. Fail. Anal.* **2022**, *132*, 105899. [[CrossRef](#)]
12. Pouranvari, M.; Marashi, S.P. Critical review of automotive steels spot welding: Process, structure and properties. *Sci. Technol. Weld. Join.* **2013**, *18*, 361–403. [[CrossRef](#)]
13. Soomro, I.A.; Pedapati, S.R.; Awang, M. A review of advances in resistance spot welding of automotive sheet steels: Emerging methods to improve joint mechanical performance. *Int. J. Adv. Manuf. Technol.* **2022**, *118*, 1335–1366. [[CrossRef](#)]
14. Shen, Z.; Ding, Y.; Gerlich, A.P. Advances in friction stir spot welding. *Crit. Rev. Solid State Mater. Sci.* **2020**, *45*, 457–534. [[CrossRef](#)]
15. Wagare, V. Fatigue life prediction of spot welded joints: A review. In *Proceedings of Fatigue Durability and Fracture Mechanics*; Springer: Berlin/Heidelberg, Germany, 2018; pp. 445–455.
16. Dassault, S. *Abaqus 6.14 Documentation*; Simulia Systems: Providence, RI, USA, 2014.
17. Dincer, S.A. A Comparative Study on the Finite Element Models for spot Welds and Their Verification. Master's Thesis, Istanbul Technical University, Beyoğlu, Turkey, 2005.
18. Gupta, R.S.; Xin, H.; Veljkovic, M. Fatigue crack propagation simulation of orthotropic bridge deck based on extended finite element method. *Procedia Struct. Integr.* **2019**, *22*, 283–290. [[CrossRef](#)]
19. Banerjee, P.; Sarkar, R.; Pal, T.K.; Shome, M. Effect of nugget size and notch geometry on the high cycle fatigue performance of resistance spot welded DP590 steel sheets. *J. Mater. Process. Technol.* **2016**, *238*, 226–243. [[CrossRef](#)]

Disclaimer/Publisher's Note: The statements, opinions and data contained in all publications are solely those of the individual author(s) and contributor(s) and not of MDPI and/or the editor(s). MDPI and/or the editor(s) disclaim responsibility for any injury to people or property resulting from any ideas, methods, instructions or products referred to in the content.